Ferroelectric Ceramic Materials Enable High-Performance Organic-Inorganic Composite Electrolytes in Solid-State Lithium Metal Batteries

Jing-Yuan Ma(马静媛)[1†], Yu-Li Huang(黄昱力)[2†], Han-Jie Zhou(周晗洁)[1], Yuan-Yuan Wang(王媛媛)[1], Jian-Gang Li(李建刚)[1], Xi-Qian Yu(禹习谦)[2], Hong Li(李泓)[2*], and Yan Li(李妍)[1*]

[1] *College of New Materials and Chemical Engineering, Beijing Institute of Petrochemical Technology, Beijing 102627, China*

[2] *Institute of Physics, Chinese Academy of Sciences, Beijing 100190, China*

(Received 27 March 2024; accepted manuscript online 20 July 2024)

Compared to commercial lithium-ion batteries, all-solid-state batteries can greatly increase the energy density, safety, and cycle life of batteries. The development of solid-state electrolyte with high lithium-ion conductivity and wide electrochemical window is the key for all-solid-state batteries. In this work, we report on the achievement of high ionic conductivity in the PAN/$LiClO_4$/$BaTiO_3$ composite solid electrolyte (CSE) prepared by solution casting method. Our experimental results show that the PAN-based composite polymer electrolyte with 5 wt% $BaTiO_3$ possesses a high room-temperature lithium-ion conductivity (9.85×10^{-4} S·cm^{-1}), high lithium-ion transfer number (0.63), wide electrochemical window (4.9 V vs Li^+/Li). The Li|Li symmetric battery assembled with 5 wt% $BaTiO_3$ can be stably circulated for 800 h at 0.1 mA·cm^{-2}, and the $LiFePO_4$|CSE|Li battery maintains a capacity retention of 86.2% after 50 cycles at a rate of 0.3 C. The influence of $BaTiO_3$ ceramic powder on the properties of PAN-based polymer electrolytes is analyzed. Our results provide a new avenue for future research in the all-solid-state lithium battery technology.

DOI: 10.1088/0256-307X/41/7/078202

Due to its high energy density, wide operating voltage range and long cycle life, commercial lithium-ion batteries are widely used in various fields such as portable electronic equipment, new energy vehicles and power grid storage.[1,2] However, batteries with liquid electrolytes have poor mechanical performance and safety hazards such as burning in the case of overheating, overcharging, and short circuits due to the volatilization of liquid solvents.[3–6] In addition, because the electrochemical window of organic electrolytes is relatively narrow, the unstable interfacial phase generated at the interface between the positive and negative electrodes will result in the continuous decomposition of the organic electrolyte and shortening of the cycling life of the battery when the oxidation and reduction reactions occur at voltages above 4.2 V or lower than 1.2 V. Thus, all solid-state batteries employing the solid-state electrolyte (SSE) materials with high power, high energy density, and high safety are considered as the ideal next-generation battery technology.[7]

Currently, the solid electrolyte materials under developments mainly include oxides, sulfides, chlorides, polymers, and composite solid electrolyte (CSE) materials. The three former inorganic solid electrolytes usually possess higher room-temperature lithium-ion conductivity. For example, the conductivity of sulfide electrolytes can exceed that of existing organic electrolytes.[8] However, the sulfide and chloride materials are expensive and sensitive to moisture, resulting in high processing costs. The oxide solid electrolyte materials require high-temperature sintering, making it difficult to prepare ultrathin electrolyte films. In contrast, polymer solid electrolytes have the merits of low cost and easy to process, but their room-temperature conductivity is only about 10^{-5}–10^{-4} S·cm^{-1} [9,10] due to the crystallization of polymer molecules. Such a drawback can be effectively overcome[11–15] by adding inorganic ceramic fillers, which inhibit the crystallization and enhance the surface interactions between polymer and ceramic powders.

Among the inorganic ceramic fillers, the ferroelectric materials have attracted considerable attention since their spontaneous polarization can promote the dissipation of lithium salts in polymer solid electrolytes and increase the carrier concentration[16,17] in addition to inhibit crystallization. Zhang and coworkers[18] prepared PEO/$BaTiO_3$ CSE with different particle sizes and concentrations using the solution casting method. Their results show that the best performance is achieved with 8 wt% $BaTiO_3$(5 nm), and the ionic conductivity can be enhanced to 2.2×10^{-5} S·cm^{-1} at 25°. Through the analysis of Fourier transform infrared (FT-IR) spectra, they concluded that the surface groups of $BaTiO_3$ particles interact with PEO chains and lead to the weakening of the complexation between Li ions and O atoms. Recently, Guo and coworkers[19] studied the dissociation mechanism of lithium bis(fluorosulfonyl)imide (LiFSI) induced by $BaTiO_3$ ferroelectric filler in $BaTiO_3$-PVDF electrolyte (PVDF: polyvinylidene fluoride) and found that the {100} plane of tetragonal-$BaTiO_3$ exhibits a significant ability to dissociate lithium salts and accumulate anions, which is due to the surface absorption of FSI^- formed by the bind-

†These authors contributed equally to this work.
*Corresponding authors. Email: yanli@bipt.edu.cn; hli@iphy.ac.cn
© 2024 Chinese Physical Society and IOP Publishing Ltd

ing between O in FSI^- and Ti in tetragonal $BaTiO_3$. The introduction of oxygen vacancies in tetragonal $BaTiO_3$ enhances the spontaneous polarization of the fillers, further increasing the dissociation degree of lithium salts and giving rise to an ionic conductivity of $8.4 \times 10^{-4}\,\mathrm{S{\cdot}cm^{-1}}$ at 25 ℃.

In addition to the above CSE, we turn our attention to another promising polymer solid electrolyte, polypropylene (PAN), which shows excellent characteristics such as heat resistance, high tensile strength, and oxidation resistance.[20] The nitrile group (C≡N) in PAN-based solid electrolyte has extremely high dipole moment, strong electron adhesion ability, and high electrochemical stability.[21] N atoms in the nitrile group can provide lonely pairing electrons and have a low interaction with lithium ions, leading to complexation.[22] They also have high antioxidant capacity, which can be matched with high-voltage positive materials. However, the ionic conductivity is relatively low at the room temperature, and the reaction between C≡N and lithium metal forms a passivation layer, which increases resistance of the battery. Previous studies on the PAN-based polymer electrolytes mainly focused on gel-shaped electrolytes containing liquid plasticizers,[23–25] while the research on the PAN/$BaTiO_3$ CSE was quite limited.

In this work, we prepared a series of PAN/$LiClO_4$/$BaTiO_3$ CSEs by using the solution casting method, and experimentally investigated the influence of $BaTiO_3$ content on the electrochemical and physical properties, including ionic conductivity, electrochemical window, mechanical properties, and all-solid-state battery performance. The results show that the addition of ferroelectric $BaTiO_3$ fillers can effectively improve the lithium-ion conductivity of PAN-base CSEs, for which the 5 wt% $BaTiO_3$ can enhance room-temperature conductivity up to $9.85 \times 10^{-4}\,\mathrm{S{\cdot}cm^{-1}}$. The interaction between $BaTiO_3$ and polymer electrolytes also greatly enlarges the lithium-ion transfer number (0.63) and the electrochemical window (4.9 V vs Li^+/Li) of the composite electrolyte. Moreover, the PAN/$LiClO_4$/$BaTiO_3$ CSEs exhibit excellent capability to inhibit the formation and growth of lithium dendrites in all-solid-state Li|Li symmetric batteries and $LiFePO_4$|Li batteries, thus greatly boosting the cycle stability of the batteries.

Experimental. The CSE membrane was prepared with the solution casting method. Before the experiment, $LiClO_4$ was dried in vacuum for 24 h at 140 ℃. $LiClO_4$ of 0.75 g was dissolved in N,N-dimethylacetamide (DMF) with intense stirring for 10 h. Then the different amounts of $BaTiO_3$ (Macklin) powders were added to the solution and dispersed by ultrasonic treatment for 15 min and magnetically stirred to obtain the homogeneous solution. Finally, we put PAN (Macklin, MW: 150000) into the above solution with a mass ration of $\mathrm{PAN}:\mathrm{LiClO_4} = 2:1$, and heated the mixture at 70 ℃ for 10 h with continuous stirring. The resultant solution was cast into a PVDF mold and dried at room temperature to remove the solvent. The average thickness of CSE membrane is approximately 10 μm.

The phase analysis of PAN/$LiClO_4$/$BaTiO_3$ CSE membranes was carried out by using x-ray diffraction (XRD, Bruker D8) in the 2θ range of 30–80° with Cu K_α radiation. The chemical interaction between the filler and the polymer matrix was studied by the FT-IR spectrometer (NICOLET 6700) and XPS (Nexsa G2) spectra. The thermal stability of the CSE membranes was measured with a thermogravimetric analyzer (TG) (HITACHI STA200) under N_2 atmosphere at a heating rate of 10°/min from room temperature to 800 ℃.

The ionic conductivity was investigated by electrochemical impedance spectroscopy (EIS) and recorded by CHI660E (Chenhua, China) with an AC amplitude of 10 mA within the frequency range from 0.1 Hz to 1 MHz. The electrochemical stability was shown by linear sweep voltammetry (LSV) at a scan rate of $1\,\mathrm{mV{\cdot}s^{-1}}$ from open circuit voltage to 6 V. The cycling properties were tested using a battery test system (CT3002A, LAND, China).

Characterization. Figure 1(a) shows the XRD spectra of PAN, $LiClO_4$, PAN/$LiClO_4$, and PAN/$LiClO_4$/5 wt% $BaTiO_3$ (CSE) together with the calculated peak positions of $BaTiO_3$ (PDF #31-0174) shown at the bottom. As can be seen, the diffraction peaks of CSE correspond one-to-one to those of each constituent substances, and no other impurities appear. It is noted that, after the addition of $BaTiO_3$, the peak intensity of both PAN and $LiClO_4$ decreases significantly, especially the main peak around 32°, which indicates that the combination of $BaTiO_3$ with PAN inhibits the crystallization of PAN and increases the dissolution of lithium salt $LiClO_4$. This in turn would help to increase the concentration of lithium ions and improve the conductivity of the composite electrolyte.

To substantiate the above XRD results and to further characterize the effect of $BaTiO_3$ filler, we measured and compared the FT-IR spectra of PAN/$LiClO_4$ and PAN/$LiClO_4$/5 wt% $BaTiO_3$ CSEs. As shown in Fig. 1(b), their spectra are similar to each other, with characteristic peaks mainly related to the PAN and $LiClO_4$ groups. The absence of new vibration absorption peaks further confirms that the CSE has been successfully prepared without introducing additional impurities. According to Refs. [26–28], the peaks in the range 600–650 $\mathrm{cm^{-1}}$ are associated with the dissociation of $LiClO_4$, with free ClO_4^- at 624 $\mathrm{cm^{-1}}$ and paired ClO_4^- at 635 $\mathrm{cm^{-1}}$. As shown in Fig. 1(b), the intensity of these two peaks is weakened upon the addition of $BaTiO_3$, which means that the spontaneous polarization of $BaTiO_3$ can not only have the ability to dissociate lithium salt but also accumulate ClO_4^- anions, resulting in the decrease of number of free ClO_4^-. The peaks in the range of 2200–2300 $\mathrm{cm^{-1}}$ correspond to the C≡N stretching vibration of PAN. After adding 5 wt% $BaTiO_3$, this peak is slightly weakened and small bulges appear on the shoulders, which should be caused by the fact that the addition of $BaTiO_3$ weakens the interaction between Li^+ and C≡N groups. This in turn can facilitate the transport of lithium ions in the PAN polymers. In addition, a peak was observed at 1660 $\mathrm{cm^{-1}}$, which is the C=O vibration peak of DMF, indicating the presence of DMF solvent residue in the composite electrolyte membrane. The intensity of this peak keeps unchanged after the addition of $BaTiO_3$, indicating that the interaction between C=O and Li^+ in DMF did not change. This result is similar to those obtained in PAN/$LiClO_4$ containing Al_2O_3 and PAN/$LiClO_4$

containing SAP CSEs.[3,9]

Figure 1(c) shows the TG curves of PAN/$LiClO_4$ and PAN/$LiClO_4$/5 wt% $BaTiO_3$ membranes. As the temperature increases, the weight begins to decrease due to the thermal volatilization of water, DMF, and other substances adsorbed on the surface of the membranes. Significant weight loss occurs at 250°–350° due to the thermal decomposition of PAN and $LiClO_4$. As shown in Fig. 1(c), the thermal decomposition temperature of PAN is about 280°. In comparison, the addition of $BaTiO_3$ slightly increases the decomposition temperature of the CSE. This indicates a better thermal stability of the CSE membrane upon the addition of $BaTiO_3$. In addition, TG measurements also indicate the presence of DMF residues in the CSE, the complete removal of the DMF solvent in PAN solid polymer electrolyte (SPE) is generally considered challenging. The TG results demonstrate that the residual DMF content remains approximately 12%, irrespective of the presence or absence of $BaTiO_3$ filler. This means that for electrolytes containing or not containing $BaTiO_3$ fillers, the plasticizing effect generated by residual solvents should be similar.

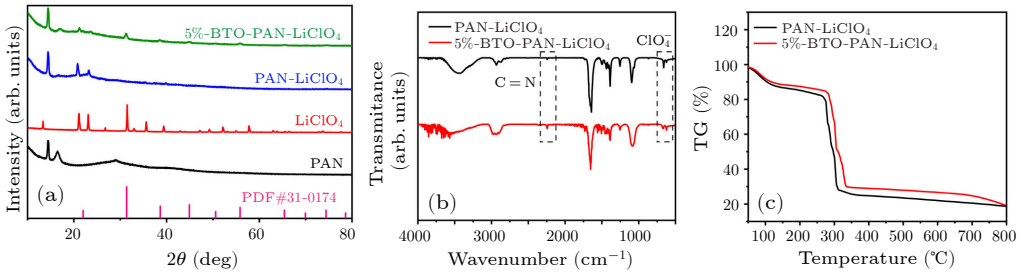

Fig. 1. (a) X-ray diffraction (XRD) pattern, (b) FT-IR spectra, (c) thermal stability of PAN/$LiClO_4$ and PAN/$LiClO_4$/$BaTiO_3$ CSEs.

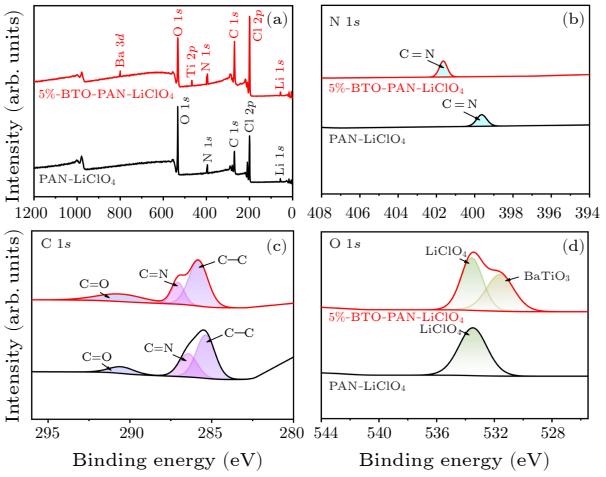

Fig. 2. XPS spectra of PAN/$LiClO_4$ and PAN/$LiClO_4$/$BaTiO_3$ CSEs.

To further analyze the elemental composition, chemical valence states, and electronic structure of CSE, we conducted XPS measurements. As shown in Fig. 2, PAN mainly contains C, H, O, and N, while the spectra of Ba and Ti appear in the entire spectrum when the $BaTiO_3$ is added. In the N 1*s* spectrum, the peak of PAN/$LiClO_4$ membrane at 399.6 eV is attributed to the C≡N bond in the PAN, while with the addition of $BaTiO_3$, the C≡N in PAN shifts towards higher binding energy, indicating that the strong polarity of $BaTiO_3$ stabilizes the C≡N chain segments in PAN. According to the Lewis acid-base interaction theory, the acidic or alkaline groups on the surface of the filler will interact with lithium salts, promoting their decomposition and leading to an increase in free oxygen near the interface.[21,29] From the O 1*s* spectrum, all O atoms come from $LiClO_4$ before the addition of $BaTiO_3$. After the addition of $BaTiO_3$, an additional O peak appears, indicating that $BaTiO_3$ has been successfully added.

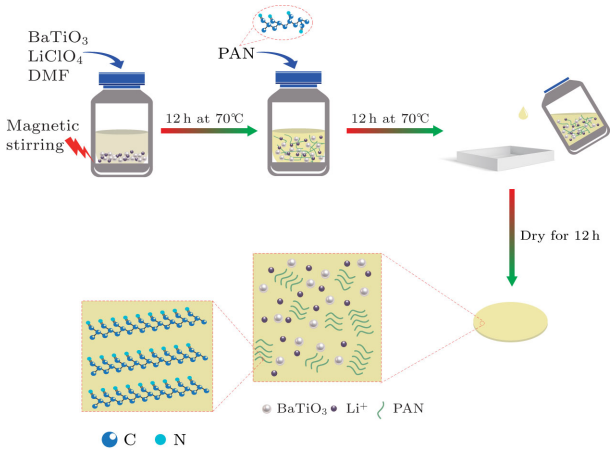

Fig. 3. Schematic illustration of the effect of $BaTiO_3$ in CSE.

The above analyses of XRD, FT-IR and XPS data demonstrate that the addition of $BaTiO_3$ can greatly affect the arrangement of PAN chain segments. In pure PAN/$LiClO_4$ membrane, the orientation of PAN segments is random, but the strong polarization center of $BaTiO_3$ in PAN/$LiClO_4$/5 wt% $BaTiO_3$ membrane causes a local regular arrangement of PAN segments through the interaction with the nitrile group in PAN, which will facilitate the transport of Li^+. The schematic diagram is shown in Fig. 3.

Electrochemical Measurements. The Li-ion conductivities of PAN/$LiClO_4$/x wt% $BaTiO_3$ (x = 0, 5, 8) CSE membranes loading in SS|CSE|SS cells were studied using electrochemical impedance spectroscopy (EIS) at temperatures ranging from 30° to 80°. As shown in Figs. 4(a) and 4(b), the conductivity of electrolyte without $BaTiO_3$ loading is only 5.58×10^{-5} S·cm^{-1} at 30°, while the conductivity increases to 9.85×10^{-4} S·cm^{-1} at 30° with 5 wt% $BaTiO_3$ addition. As the temperature increases, it reaches 3.41×10^{-3} S·cm^{-1} at 80°. For the

PAN/$LiClO_4$/8 wt% $BaTiO_3$ CSE membrane, the ionic conductivity is 2.74×10^{-4} S·cm^{-1} at 30°. This means that, with the increasing concentration of $BaTiO_3$ filler to 8 wt%, the ionic conductivity is lower than that of PAN/$LiClO_4$/5 wt% $BaTiO_3$ CSE membrane. This is due to the fact that excessive inorganic fillers will aggregate in the PAN matrix, hindering the lithium-ion transport. Therefore, in the following, we will concentrate on the PAN/$LiClO_4$/5 wt% $BaTiO_3$ CSE membrane. Figure 4(c) shows the Arrhenius plot of PAN/$LiClO_4$/$BaTiO_3$ CSE. The activation energies (E_a) of the CSEs decrease from 0.38 eV to 0.24 eV upon the addition of 5 wt% $BaTiO_3$, which effectively reduces the migration barrier of lithium ions in solid electrolytes.

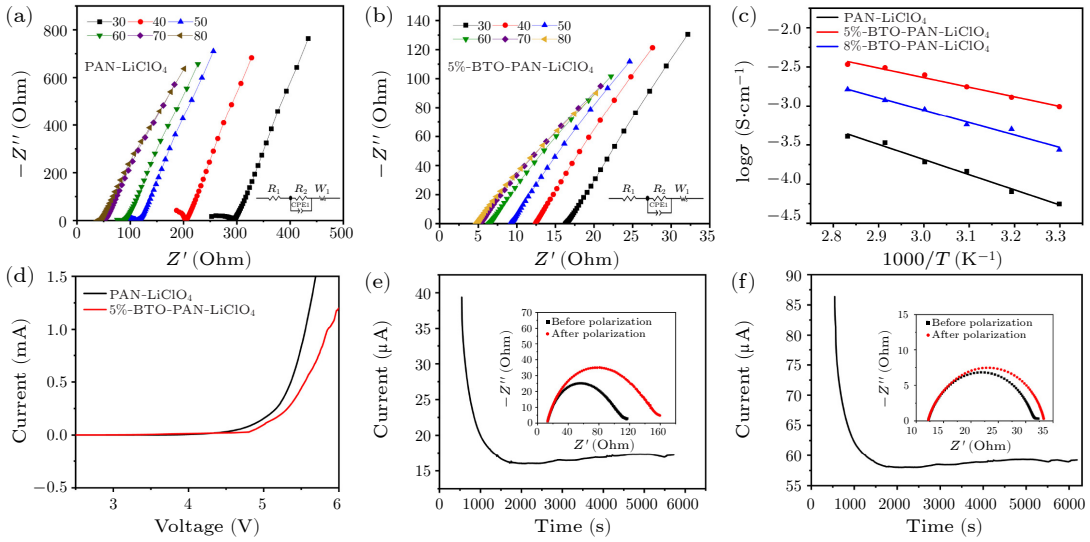

Fig. 4. [(a), (b)] Impedance diagram of SS|SPE|SS of PAN/$LiClO_4$/$BaTiO_3$ CSE with x wt%$BaTiO_3$ (x = 0, 5) added at different temperatures; and (c) its Arrhenius diagram. (d) LSV curve of PAN/$LiClO_4$/$BaTiO_3$ CSE. [(e), (f)] Time-dependent response of dc polarization in a symmetric Li|CSE|Li cell. Inset: impedance spectra before (black dots) and after (red dots) polarization.

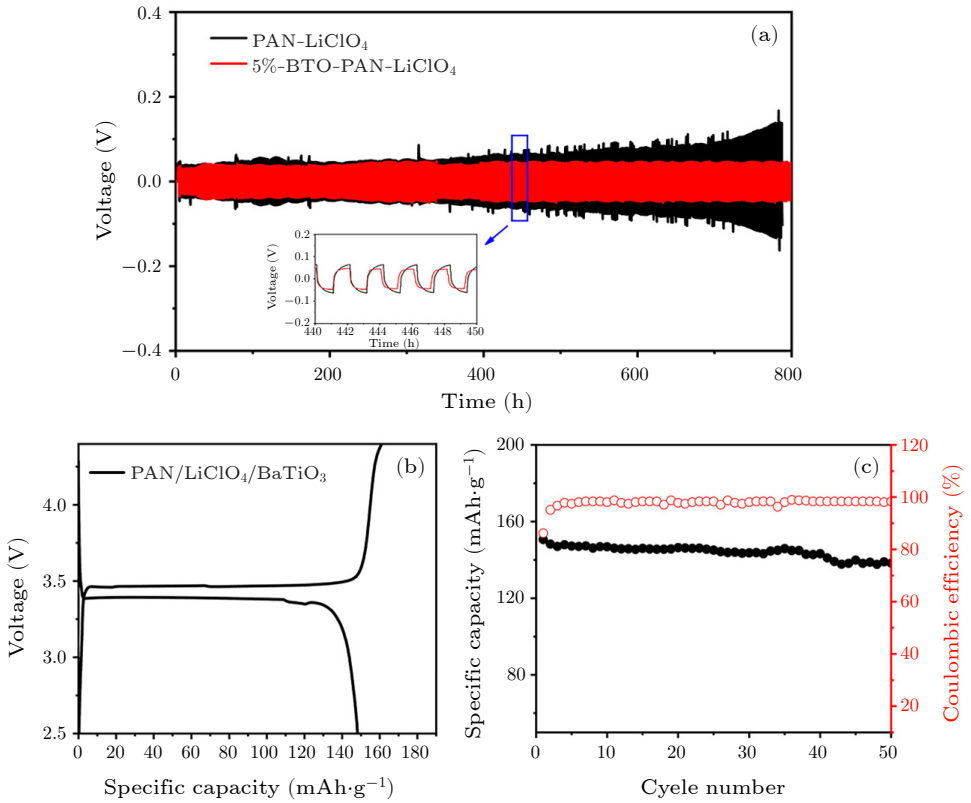

Fig. 5. (a) Voltage–time profiles of the Li|CSE|Li cell; (b) cycling performance of LFP|CSE|Li at a rate of 0.3 C; (c) first cycle charge-discharge curve of LFP|CSE|Li at a rate of 0.3 C.

The electrochemical stability window of the membrane with various $BaTiO_3$ loading was studied at room temperature using linear sweep voltammetry (LSV). As shown in Fig. 4(d), the LSV of the membrane without $BaTiO_3$ loading indicates that the oxidation of the polymer matrix occurs at 4.6 V. On the other hand, the CSE membrane with 5 wt% $BaTiO_3$ is stable up to 4.9 V versus Li^+/Li.

The lithium-ion transference number is a key parameter for the CSE. We can obtain the lithium-ion transference number t_{Li^+} of the CSE membrane at room temperature with a symmetric Li|CSE|Li cell using the equation $t_{Li^+} = \frac{I_S(\Delta V - I_0 R_0)}{I_0(\Delta V - I_S R_S)}$, where ΔV is the applied voltage, $I_0(R_0)$ and $I_S(R_S)$ are the initial and steady current (resistance), respectively. The t_{Li^+} value of the CSE with 5 wt% $BaTiO_3$ is 0.63, which is much larger than $t_{Li^+} = 0.33$ of the PAN/$LiClO_4$. This indicates that the addition of $BaTiO_3$ can promote the chain segment interaction of PAN. In addition, according to the Lewis acid-base theory, $BaTiO_3$ particles with ferroelectricity can attract anions in the lithium salts, and more lithium ions can move freely, thereby improving the t_{Li^+} and the performance of CSE.

The symmetrical Li|CSE|Li cells were assembled to evaluate the electrochemical stability of CSE against Li metal anode during periodical charging and discharging with a constant current density of 0.1 $mA{\cdot}cm^{-2}$. As shown in Fig. 5(a), a symmetrical battery with 5 wt% $BaTiO_3$ CSE exhibits a very stable voltage response of 0.03 V during 800 h of cycling, indicating that the process of lithium plating and stripping at the interface between electrolyte and lithium metal is uniform and stable. On the contrary, the voltage of the symmetric battery with PAN/$LiClO_4$ membrane began to fluctuate after 500 h, and the polarization voltage gradually increases, exhibiting larger overpotential and poor stability. This indicates that the $BaTiO_3$ filler plays a positive role in inhibiting the growth of lithium dendrites and thus improving the interface stability. This is beneficial for achieving a longer and more stable cycle life of the battery.

We assembled and tested the performance of $LiFePO_4$|CSE|Li solid-state batteries operated at 30° and 0.3 C rate. Figure 5(b) shows that the discharge specific capacity in the early stage of the cycle reached 151.4 $mAh{\cdot}g^{-1}$. After 50 cycles, the discharge specific capacity is reduced to 130.5 $mAh{\cdot}g^{-1}$, with a Coulombic efficiency of 86.2%, Fig. 5(c). The long cycle performance still needs to be further improved. The observed decay of capacity may be caused by the interfacial instability between the CSE and the cathode, which also needs to be optimized in the future work.

In summary, we have prepared the CSE membranes of PAN/$LiClO_4$/5 wt% $BaTiO_3$ with high lithium-ion conductivity at room temperature using the solution casting method. The FT-IR spectrum and XPS results prove that the interaction between the ferroelectric filler $BaTiO_3$ and polarized PAN chain change the arrangement of PAN chain segments from random orientation to local regular orientation, which is conducive to the transference of lithium ions. The CSE membrane exhibits high ionic conductivity (9.85×10^{-4} $S{\cdot}cm^{-1}$ at room temperature), rapid lithium-ion transference number (0.63) and wide electrochemical stable window (4.9 V). Finally, the Li|Li symmetrical battery remains stable upon cycling for 800 h at 0.1 $mA{\cdot}cm^{-2}$, and the $LiFePO_4$|CSE|Li battery maintains a capacity retention rate of 86.2% after 50 cycles at a rate of 0.3 C.

References

[1] Goodenough J B 2014 *Energy Environ. Sci.* **7** 14
[2] Ulissi U, Agostini M, Ito S, Aihara Y, and Hassoun J 2016 *Solid State Ionics* **296** 13
[3] Chen-Yang Y W, Chen H C, Lin F J, and Chen C C 2002 *Solid State Ionics* **150** 327
[4] Zhang Y L, Xia H L, Lin J, Chen S J, and Xu X X 2018 *Energy Storage Sci. Technol.* **7** 994
[5] Manthiram A, Yu X, and Wang S 2017 *Natl. Rev. Mater.* **2** 16103
[6] Xu R C, Wang X L, Zhang S Z, Xia Y, Xia X H, Wu J B, and Tu J P 2018 *J. Power Sources* **374** 107
[7] Chen S J, Xie D J, Liu G Z, Mwizerwa J P, Zhang Q, Zhao Y R, Xu X X, and Yao X Y 2018 *Energy Storage Mater.* **14** 58
[8] Li Y, Song S, Kim H *et al.* 2023 *Science* **381** 50
[9] Chen Y T, Chuang Y C, Su J H, Yu H C, and Chen-Yang Y W 2011 *J. Power Sources* **196** 2802
[10] Mindemark J, Lacey M J, Bowden T, and Brandell D 2018 *Prog. Polym. Sci.* **81** 114
[11] Wu I D and Chang F C 2007 *Polymer* **48** 989
[12] Zhang J, Zheng C, Lou J *et al.* 2019 *J. Power Sources* **412** 78
[13] Zheng C, Li L J, Wang K *et al.* 2021 *Batteries Supercaps* **4** 8
[14] Wang C, Yang T, Zhang W, Huang H, Gan Y, Xia Y, He X, and Zhang J 2022 *J. Mater. Chem. A* **10** 3400
[15] Yang T Q, Wang C, Zhang W K *et al.* 2022 *Rare Met.* **41** 1870
[16] Zhou J, and Fedkiw P S 2004 *Solid State Ionics* **166** 275
[17] Li Q, Imanishi N, Takeda Y, Hirano A, and Yamamoto O 2002 *Ionics* **8** 79
[18] Zhang Y, Wang X, Feng W, Zhen Y, Zhao P, Li L, and Cai Z 2019 *J. Solid State Electrochem.* **23** 749
[19] Guo S, Tan S, Ma J *et al.* 2024 *Energy Environ. Sci.* **17** 3797
[20] Hu P, Chai J, Duan Y, Liu Z, Cui G, and Chen L 2016 *J. Mater. Chem. A* **4** 10070
[21] Yu X, Li J, and Manthiram A 2020 *ACS Mater. Lett.* **2** 317
[22] Wang S H, Kuo P L, Hsieh C T, and Teng H 2014 *ACS Appl. Mater. Interfaces* **6** 19360
[23] Huang B Y, Wang Z X, Chen L Q, Xue R J, and Wang F S 1996 *Solid State Ionics* **91** 279
[24] Choe H S, Carroll B G, Pasquariello D M, and Abraham K M 1997 *Chem. Mater.* **9** 369
[25] Stone R S 1997 *J. Geophys. Res.: Atmospheres* **102** 21769
[26] Borkowska R, Reda A, Zalewska A, and Wieczorek W 2001 *Electrochim. Acta* **46** 1737
[27] Salomon M, Xu M, Eyring E M, and Petrucci S 1994 *J. Phys. Chem.* **98** 8234
[28] Wieczorek W, Lipka P, Żukowska G, and Wyciślik H 1998 *J. Phys. Chem. B* **102** 6968
[29] Fan L, Nan C W, and Zhao S 2003 *Solid State Ionics* **164** 81